SPPLEMENTARY MATERIAL

Network Pharmacology Uncovers Anti-cancer Activity of Vibsane-Type Diterpenes from *Viburnum odoratissimum*

Ying-Ying Zhang[1], Jing-Jie Chen[1], Dan-Qi Li[2], Yan-Zhang[1], Xiao-Bo Wang[1,3]*, Guo-Dong Yao[1]* and Shao-Jiang Song[1]*

[1] *School of Traditional Chinese Materia Medica, Key Laboratory of Computational Chemistry-Based Natural Antitumor Drug Research & Development, Liaoning Province, Shenyang 110016, People's Republic of China;*

[2]*Institute of Functional Molecules, Shenyang University of Chemical Technology, Shenyang 110142, People's Republic of China;*

[3]*Chinese People's Liberation Army 210 Hospital, Dalian 116021, People's Republic of China*

*Correspondence to: E-mail: songsj99@163.com (Shao-Jiang Song); guodong_yao@126.com; (Guo-Dong Yao); wxbbenson0653@sina.com (Xiao-Bo Wang)

Tel. /fax: +86 24 23986510 (Shao-Jiang Song); +86 24 23986510 (Guo-Dong Yao); +04 11 39847094 (Xiao-Bo Wang)

Network Pharmacology Uncovers Anti-cancer Activity of Vibsane-Type Diterpenes from *Viburnum odoratissimum*

Abstract

Vibsane-type diterpenes, the characteristic compounds of *Viburnum odoratissimum*, exhibited significant cytotoxicity in many cancer cells. To search for the potential target of vibsane-type diterpenes on lung cancer, we combined methods of network pharmacology prediction and experimental verification. 80 active ingredients, 23 potential targets and 39 related pathways were analysed through constructing the compound-target network and target-pathway network, and the potential target (EGFR) and key pathway (PI3K/Akt) were identified. Vibsanol C, an isolated vibsane-type diterpene with excellent cytotoxicity against lung cancer cells was chosen for further confirmation. Molecular docking study and drug affinity responsive target stability (DARTS) approach further indicated that EGFR is a direct target of Vibsanol C. Moreover, mechanistic studies revealed Vibsanol C might affect PI3K/Akt pathway by Western blot analysis. In conclusion, this study successfully predicted and confirmed the potential target of Vibsane-type diterpenes on lung cancer.

Keywords: Vibsane-type diterpenes; lung cancer; network pharmacology; drug affinity responsive target stability; epidermal growth factor receptor

List of supplementary content

Experimental

Chemicals and reagents

The dried leaves of *V. odoratissimum* were obtained from Xishuangbanna Tropical Botanical Garden (Yunnan, China) in 2014 and were identified by Professor Pan Bo (Xishuangbanna Tropical Botanical Garden, Chinese Academy of Sciences). The air-dried leaves of *V. odoratissimum* (7.3 Kg) were flash extracted third with 75% EtOH. The ethanol extract was concentrated and loaded onto a D101 macroporous resin column using an EtOH/H_2O gradient. And then separated by vacuum liquid chromatography, CHP20 CC and sephadex LH-20 column chromatography, the separation was subjected to the Silica gel column, preparative HPLC and semi-preparative HPLC to yield Vibsanol C (5 mg). The reagent was dissolved in dimethylsulfoxide (DMSO) at a stock concentration of 50 mM.

Fetal bovine serum (FBS) was purchased from Tianjin Haoyang Biotechnology Co., Ltd, (Tianjin, China). Dulbecco's modified Eagle's medium (DMEM), Phosphate balanced solution (PBS) and Antibiotics (100 U/mL penicillin, 100 μg/mL streptomycin) were purchased from HyClone, Inc (Utah, USA). EGFR, PI3K, Akt, p-Akt, p-GSK3β and β-actin and horseradish-peroxidase-conjugated secondary antibodies (goat anti-rabbit or goat anti-mouse) were purchased from Santa Cruz Biotechnology (CA, USA). PVDF membranes (0.2 μm) were purchased from Millipore (Massachusetts, USA). Coomassie blue fast staining solution were purchased from Beyotime, (Shanghai, China).

Database construction

Based on the vibsane-type diterpenes retrieved through literature, a database consisting of 80 natural products was established (**Table S1**), which was based on the reported vibsane-type diterpenes from the family *V. odoratissimum*. ChemBioDraw (http://www.cambridgesoft.com/) was used to make 3D chemical structural formulas of the ingredients, which were saved in "mol2" format.

Up to 23 protein targets (**Table S2**) related to lung cancer were obtained. The candidate proteins were data-mined from literatures and public database sources, including PubMed (www.PubMed.org), Therapeutic Targets Database (TTD;

http://bidd.nus.edu.sg/group/ttd/). The X-ray or NMR structures of the proteins for docking were downloaded from the RCSB Protein Data Bank (http://www.pdb.org/) by the following criteria: (a) the source organism is human; (b) the structure should contain an original ligand to define the active site for docking; (c) the resolution of the structure of the protein–ligand complex is below 3 Å. At the same time, the protein structures were prepared with Sybyl-X (version 2.0, TRIPOS Inc.), including addition of hydrogen atoms as well as removal of co-crystalled ligands and water molecules from the complexes.

Molecular docking

Molecular docking, which plays an important role in the rational drug design, is frequently used to predict the binding sites and binding pose(s) of drug candidates to their targets and also to estimate the binding affinity of the molecules(Kitchen et al. 2004). Surflex-Dock plug-in included in the Sybyl-X (version 2.0, TRIPOS Inc.) was used to perform molecular docking. The binding ability was evaluated using a scoring function analysis and the higher docking score represent better binding ability. For docking studies with Surflex-Dock, the ligand binding site protomol was generated using the ligand option in which the X-ray co-crystalled ligand pose was specified as references. The visualization of intermolecular forces between candidate compound and potential target was preformed on Discovery Studio 4.5 program.

Network construction and analysis

To facilitate scientific interpretation of complex relationships among the compounds, targets and pathways, the C-T network and T-P network were generated by Cytoscape 3.2.1 (http://www.cytoscape.org/), which is an open source software project for analysis and visualization of biological networks(Sheng et al. 2014).

The interaction between molecules and target proteins (docking scores greater than 6.0) were chosen to generate a C-T network in which nodes represent molecules or target proteins. For each of these 23 compounds, the top 10 targets with degree higher than 30 were selected to as the potential targets.

Cell culture

Human lung cancer A549 cells were obtained from American Type Culture

Collection (ATCC) (Manassas, VA, USA). Cells were cultured in DMEM medium (HyClone, Utah, USA) supplemented with 10% fetal bovine serum FBS (TBD, Tianjin, China), 100 units/mL penicillin, and 100 μg/mL streptomycin (HyClone, Utah, USA). Cells were incubated at 37°C with 5% CO_2 in a humidified atmosphere. All experiments were performed on logarithmically growing cells.

Target identification using drug affinity responsive target stability

A549 cells (1×10^6/mL, 2 mL) were seeded into dishes and allowed to grow for 24 h, then under standard culture conditions were treated with Vibsanol C (40 μM) in DMSO or with DMSO alone (control). At the end of 1h (treatment time), cell lysates were prepared in Cell Lysis (0.5% NP40) buffer with 1 mM PMSF (protease inhibitor) on ice for 30 min, followed by centrifugation. Protein concentration was measured with the BCA Protein Assay Kit to ensure that there was between 2.5 mg/mL and 5 mg/mL of protein. For proteolysis, each cellular lysate sample was proteolysed at room temperature for 30 min with pronase 1:2000 ratios of Pronase versus cell lysates protein concentration were used for proteolysis. Samples were loaded on SDS-PAGE and run in 1 × SDS running buffer. At the end, gels were stained with Coomassie blue(Lomenick et al. 2011).

Western blot analysis

The total cellular samples were harvested and lysed in RIPA buffer [250 mM Tris-HCl (pH 6.8), 4% SDS, 10% glycerol, 0.006% bromophenol blue, 2% β-mercaptoethanol, 50 mM sodium fluoride, and 5 mM sodium orthovanadate] and boiled for 10 min at 100 ^{o}C. Equal amount of protein (30 μg) were separated on a 10% SDS-PAGE gel and transferred to nitrocellulose membranes. The membranes were blocked with 5% BSA and probed with a primary antibody followed by the corresponding secondary antibody. Immunoreactive bands were visualized with a chemiluminescence kit (ThermoFisher, Waltham, USA) followed by incubation with HRP-conjugated secondary antibodies. The densities of protein bands were calculated by the ImageJ software (National Institutes of Health, Wayne Rasband, USA).

Statistical analysis

All results were calculated as the mean ± SD for at least three independent

experiments. Experimental data were analysed by one-way or two-way ANOVAs using GraphPad Prism version 6.0 (GraphPad Software, San Diego, CA, USA). Statistical significance was considered at $P < 0.05$.

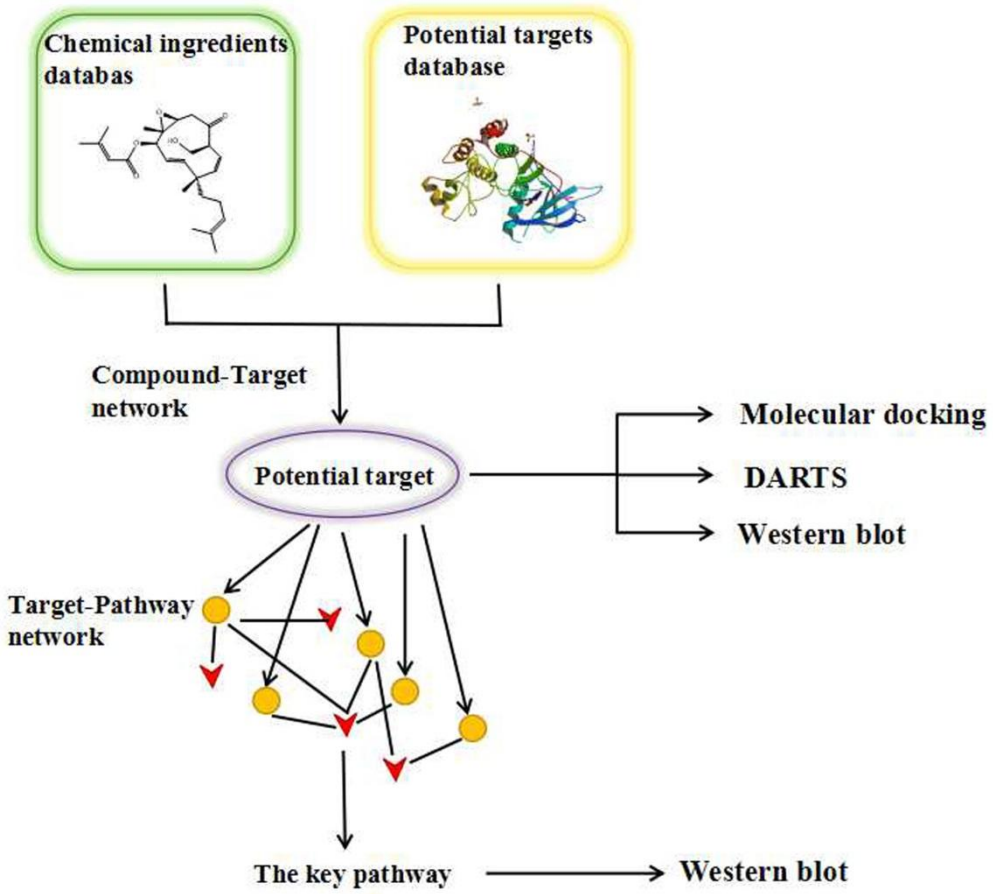

Figure S1. Process overview.

Mass Spectrum Molecular Formula Report

Analysis Info

Analysis Name	D:\Data\20151113CEYANG\VIB-41_1-E,4_01_5951.d	Acquisition Date	11/13/2015 3:43:07 PM
Method	20131026_ceyang.m	Instrument / Ser#	Bruker Customer
Sample Name	VIB-41	Operator	micrOTOF-Q 125
Comment			

Acquisition Parameter

Source Type	ESI	Ion Polarity	Positive	Set Nebulizer	1.2 Bar
Focus	Active	Set Capillary	4500 V	Set Dry Heater	180 °C
Scan Begin	50 m/z	Set End Plate Offset	-500 V	Set Dry Gas	8.0 l/min
Scan End	3000 m/z	Set Collision Cell RF	400.0 Vpp	Set Divert Valve	Source

Generate Molecular Formula Parameter

Formula, min.		
Formula, max.		
Measured m/z	Tolerance	Charge
Check Valence	Minimum	Maximum
Nirogen Rule	Electron Configuration	
Filter H/C Ratio	Minimum	Maximum
Estimate Carbon		

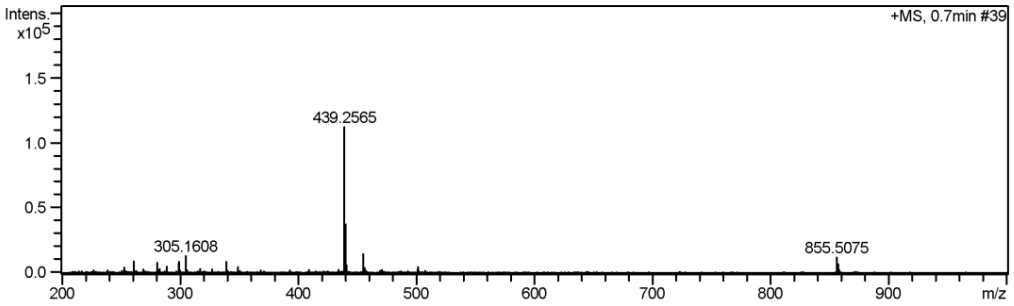

Figure S2.1 HRESIMS spectrum of **Vibsanol C**.

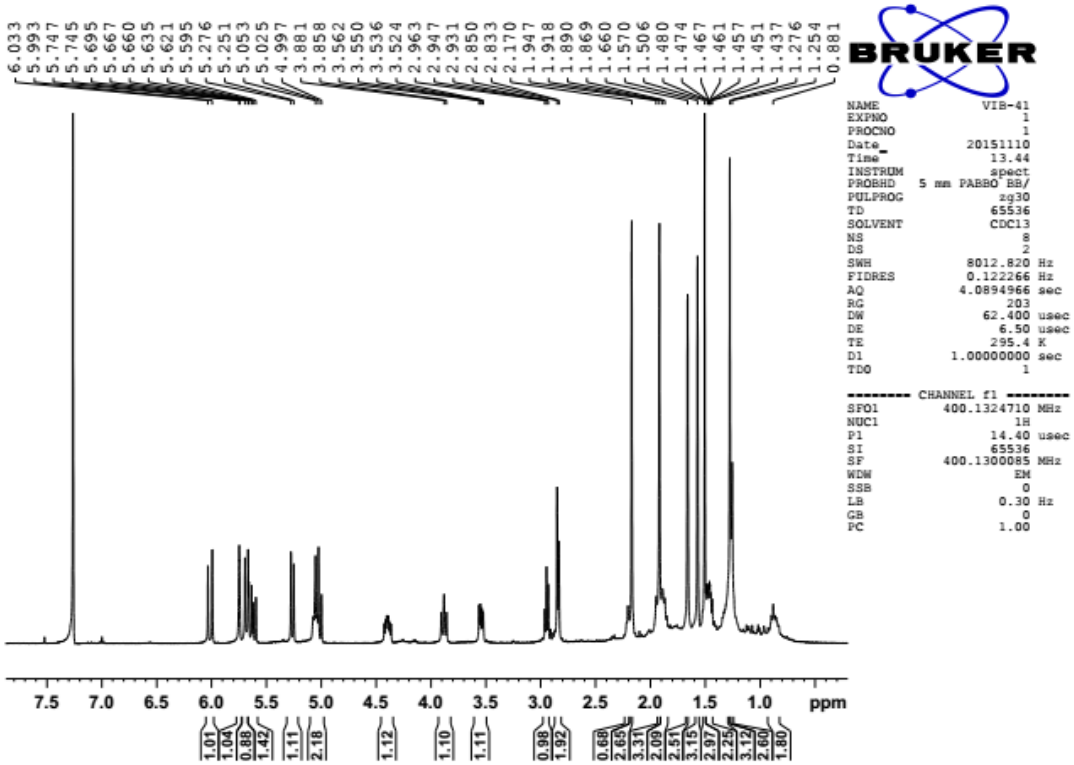

Figure S2.2 ^{1}H NMR spectrum (400 MHz, $CDCL_3$) of **Vibsanol C**.

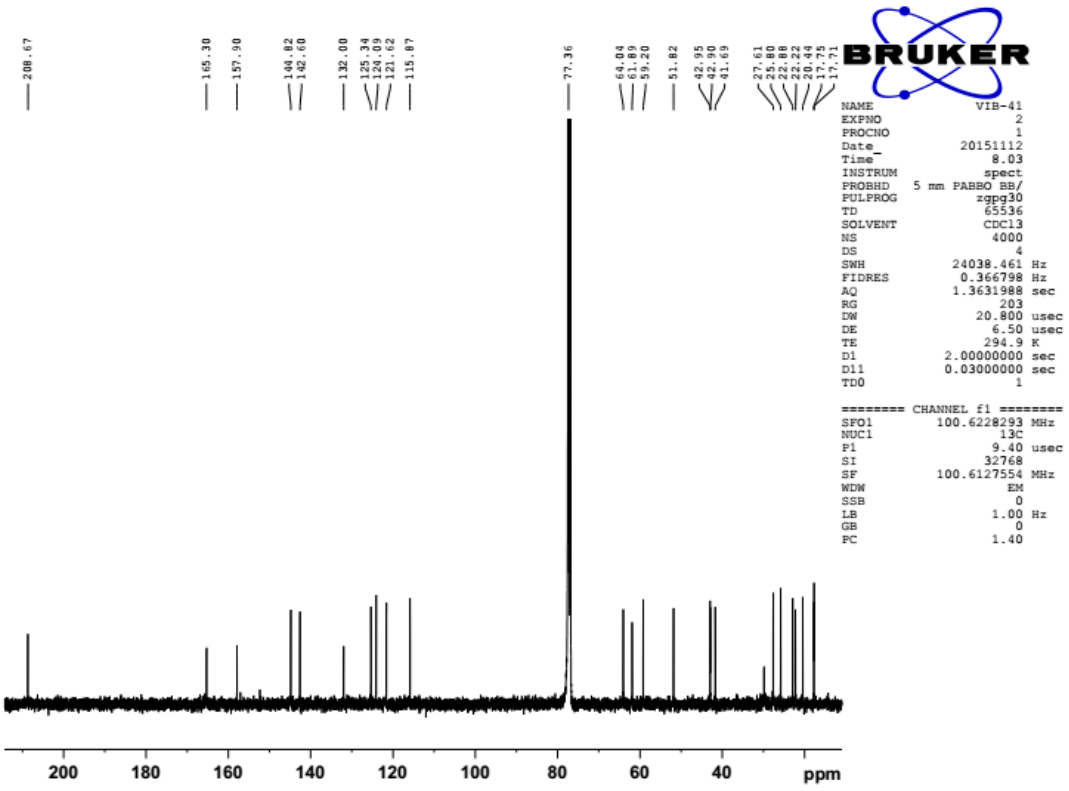

Figure S2.3 ^{13}C NMR spectrum (100 MHz, $CDCL_3$) of **Vibsanol C**.

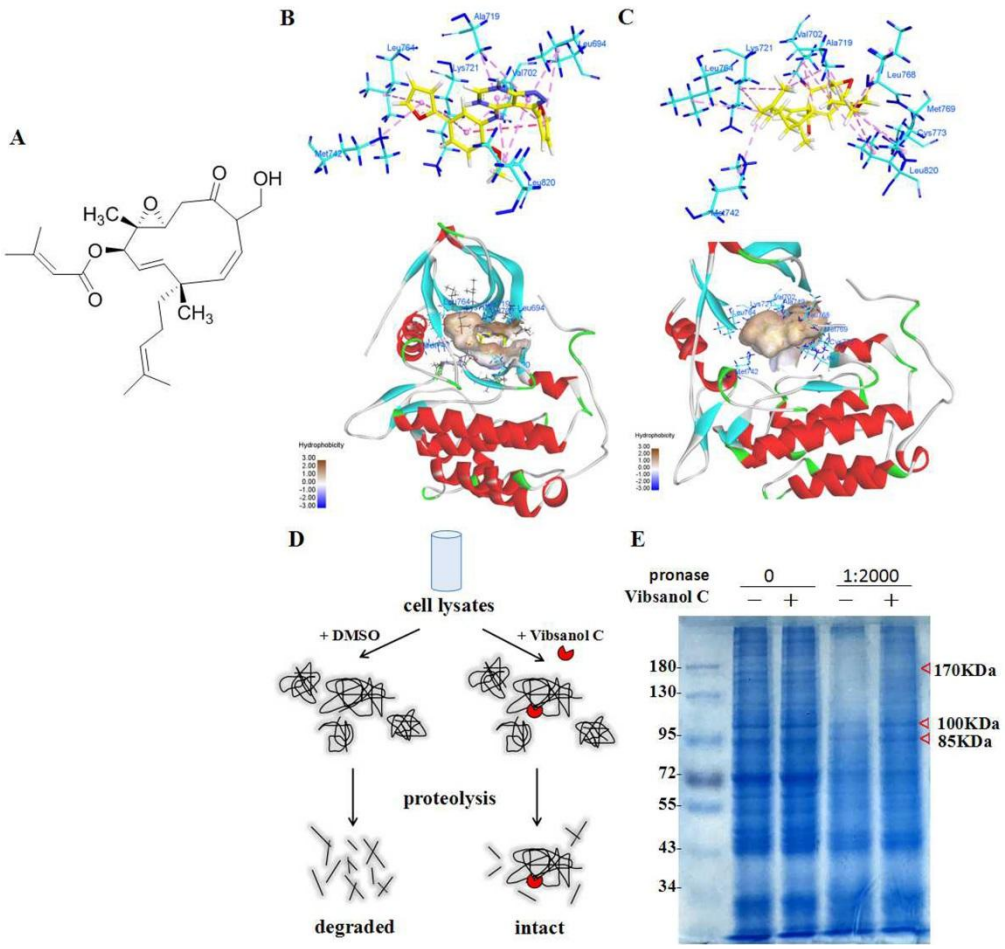

Figure S3. Identification the protein target. (A) The structure of Vibsanol C. (B) The binding mode of ligand in the active site of EGFR pocket. (C) The binding mode of Vibsanol C in the active site of EGFR pocket. Vibsanol C (yellow carbon) and amino acids residues (cyan carbon) were presented in sticks. Hydrophobic interactions were highlighted in carnation dashed lines. Hydrophobic surface in receptor residues were indicated from blue for hydrophilic to brown for hydrophobic. (D) Illustration of the DARTS method. (E)Target identification of Vibsanol C using drug affinity responsive target stability (DARTS). Red triangle flanks the protected band.

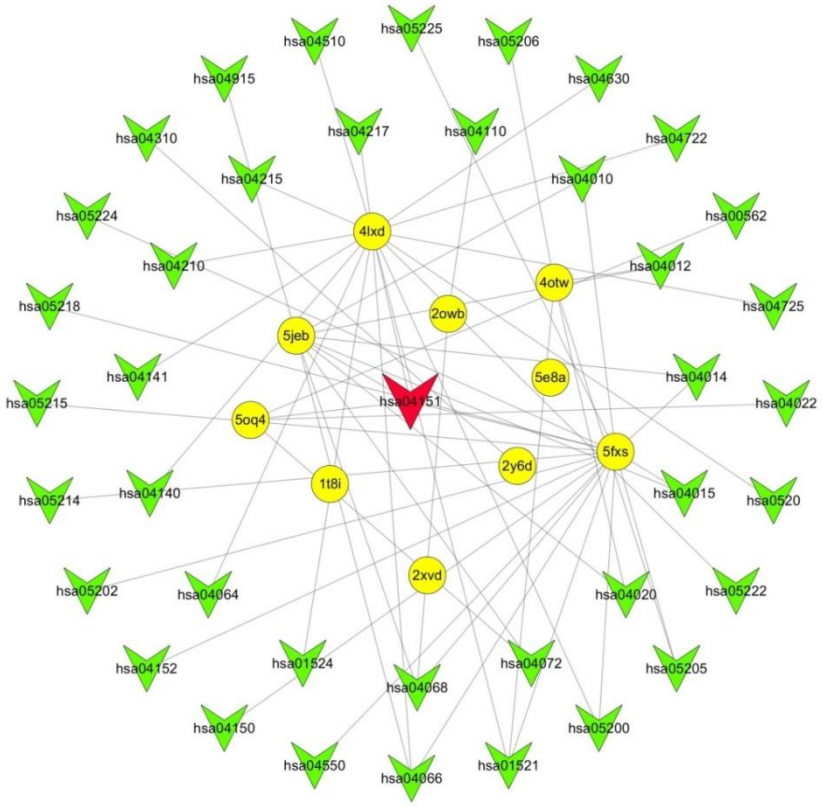

Figure S4. Target-pathway network. The yellow circles represent the targets and the red V for the most important pathways and green V for other pathways, respectively.

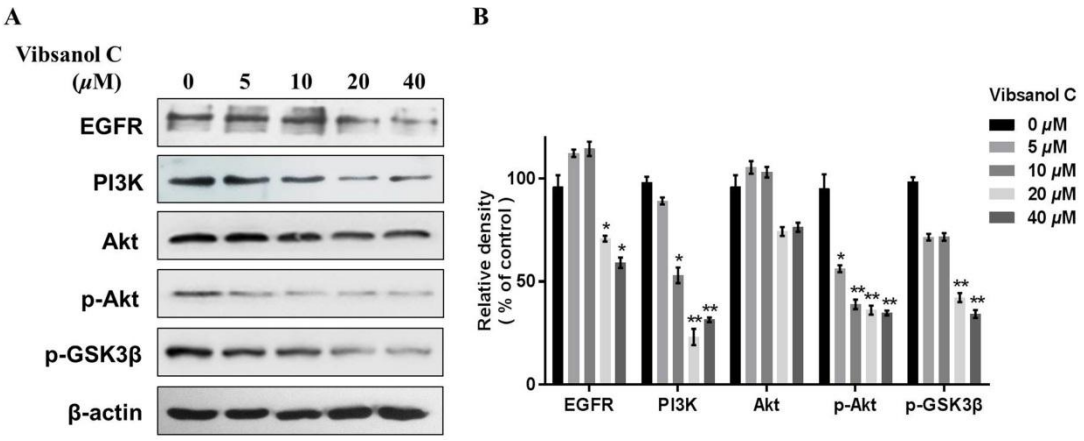

Figure S5. The expressions of EGFR, PI3K, Akt, p-Akt, p-GSK3β were detected by Western blot, respectively. β-acting was used as a loading control. The results are expressed as the mean ± SD for each group. *P<0.05; **P<0.01versus control.

The denomination and structures of the Vibsane-type diterpenes

NO	Structure	名称
1	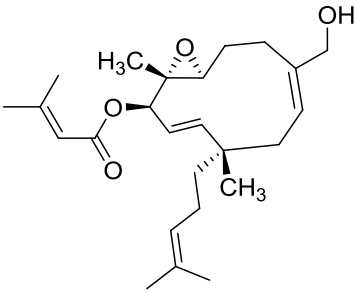	Vibsanin A
2	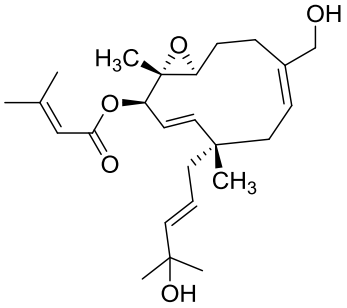	Vibsanin P
3	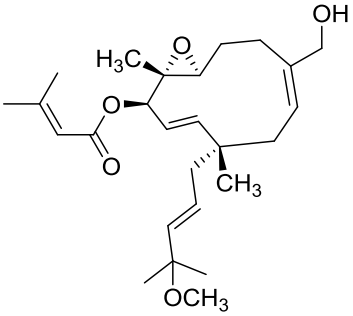	Vibsanin Q
4	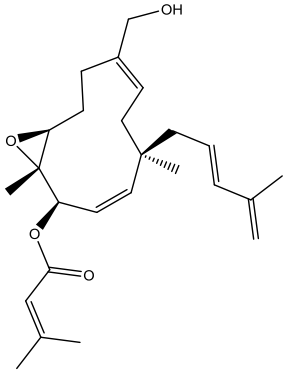	Vibsanin R

5	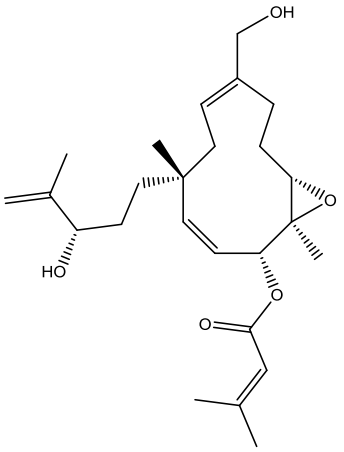	Vibsanin S
6	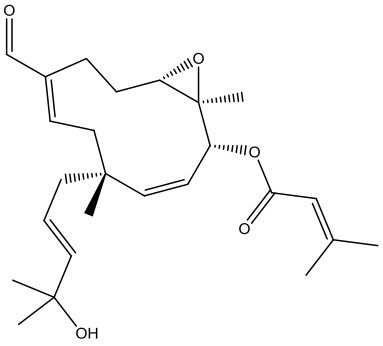	Vibsanin T
7	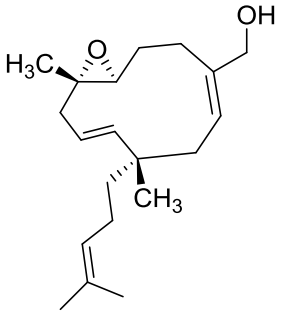	Vibsanin F
8	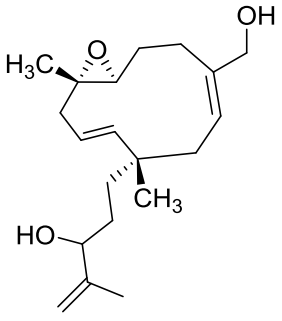	14-Hydroxyvibsanin F

9	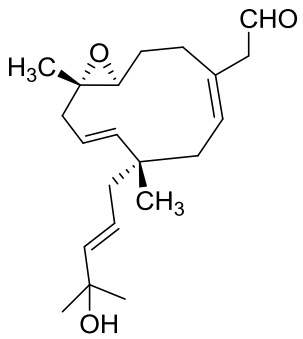	Vibsanin V
10	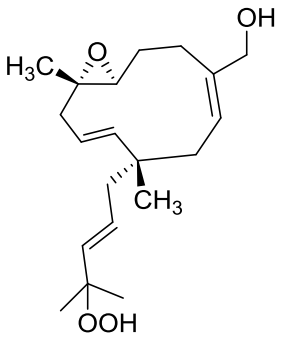	Vibsanol H
11	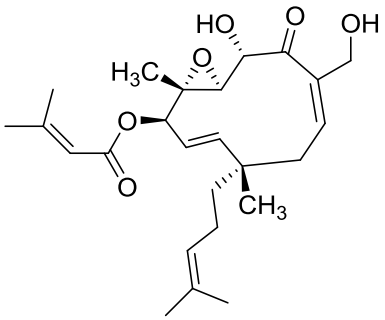	Vibsanin L
12	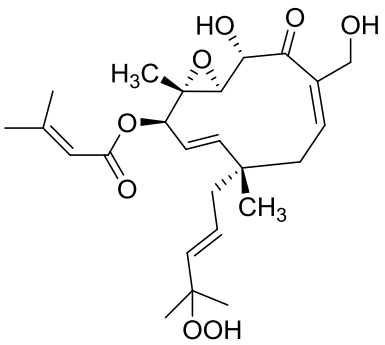	Vibsanol E
13	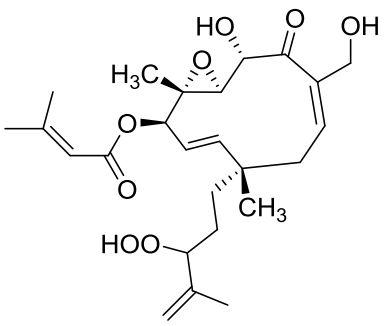	Vibsanol G

14	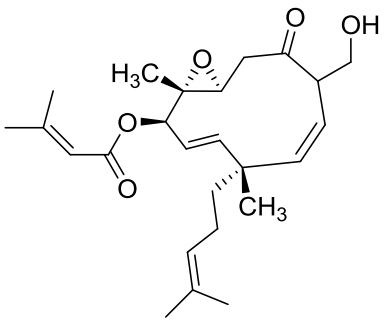	Vibsanol C
15	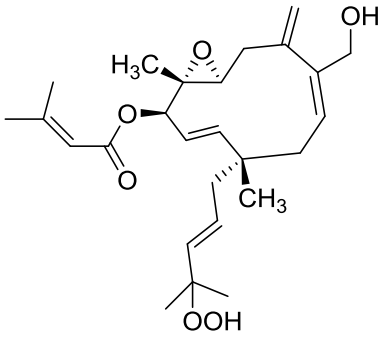	Vibsanol D
16	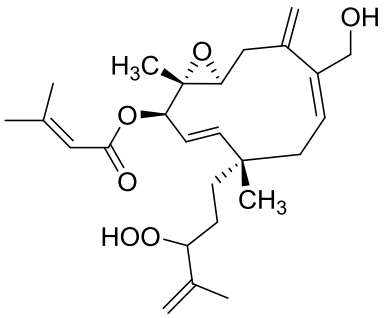	Vibsanol F
17	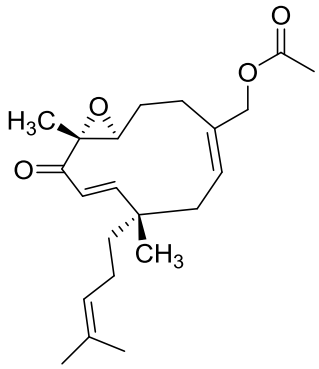	Vibsanin X
18	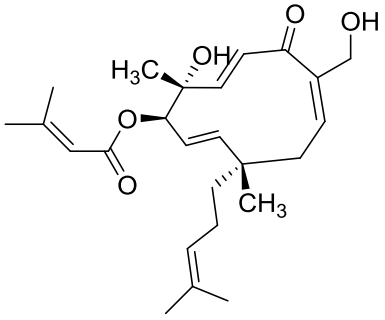	Vibsanin B

19	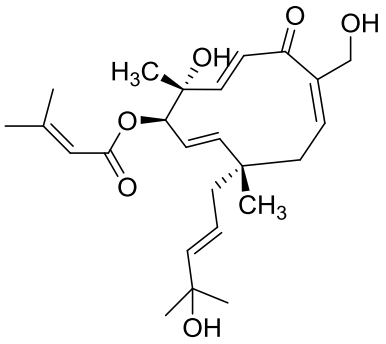	Vibsanol A
20	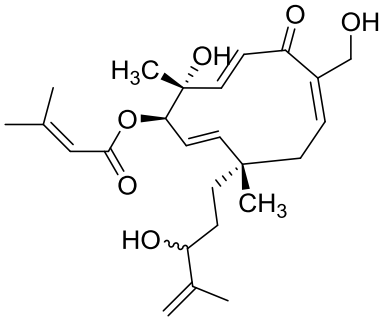	Vibsanol B
21	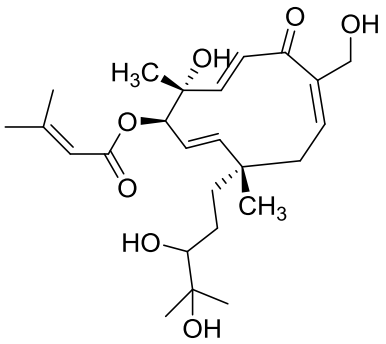	Vibsanin U
22	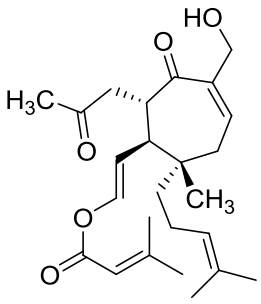	Vibsanin C
23	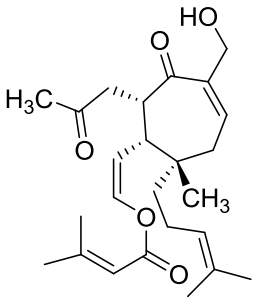	Vibsanin D

24	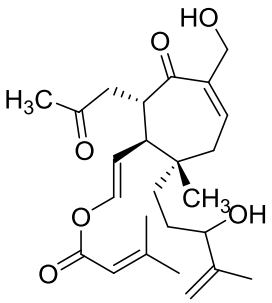	Vibsanin G
25	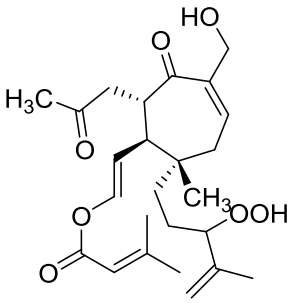	Vibsanin I
26	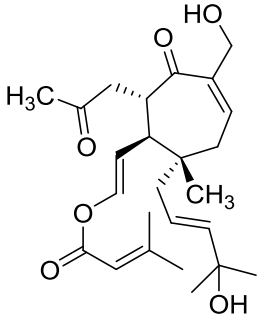	Vibsanin H
27	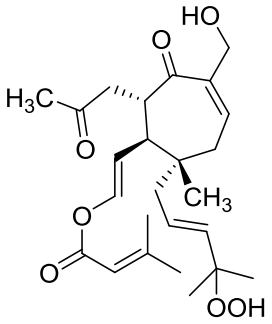	Vibsanin K
28	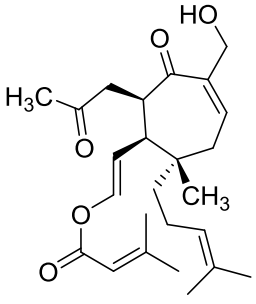	5-Epivibsanin C

29	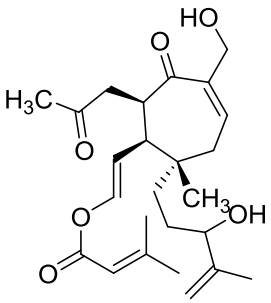	5-Epivibsanin G
30	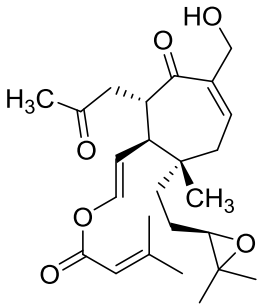	(14*R**)-14, 15-Epoxyvibsanin C
31	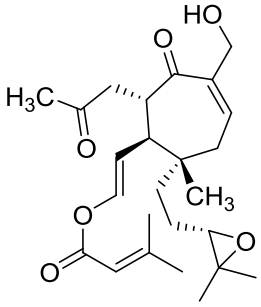	(14*S**)-14, 15-Epoxyvibsanin C
32	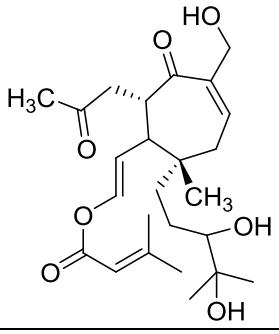	Vibsanin W
33	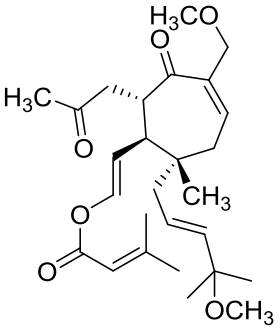	15, 18-Di-*O*-methylvibsanin H

34	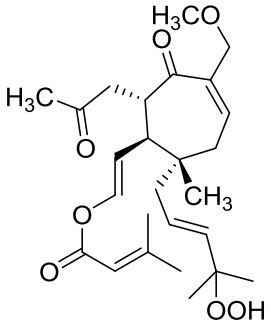	18-*O*-Methylvibsanin K
35	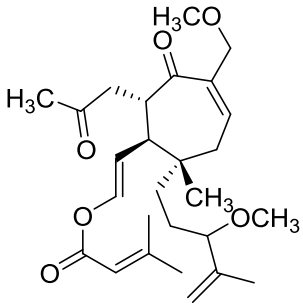	18-*O*-Methylvibsanin G
36	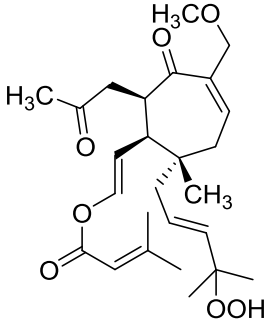	18-*O*-Methyl-5-epivibsanin K
37	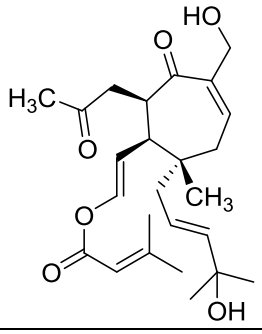	5-Epivibsanin H
38	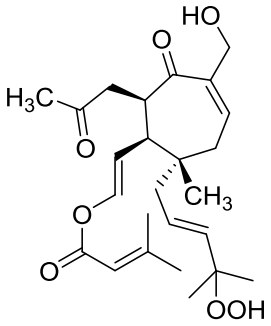	5-Epivibsanin K

39	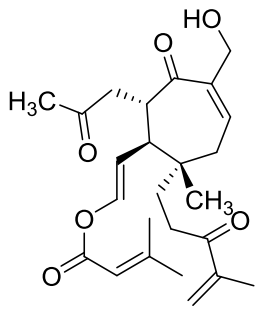	Dehydrovibsanin G
40	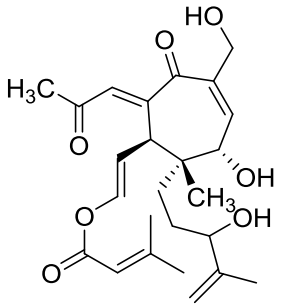	Vibsanin M
41	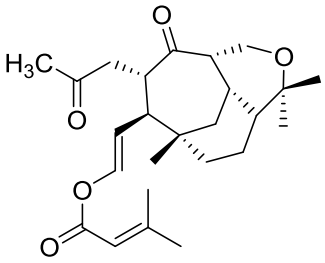	Vibsanin E
42	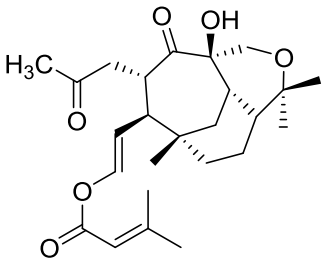	3-Hydroxyvibsanin E
43	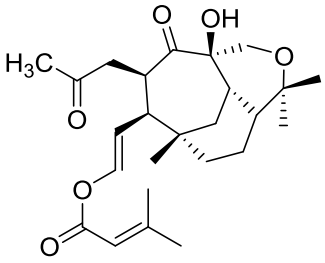	5-Epivibsanin E
44	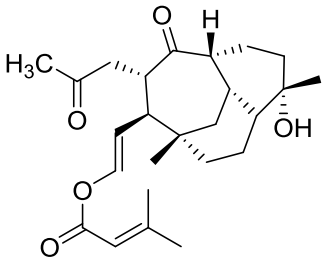	Cyclovibsanin A

45	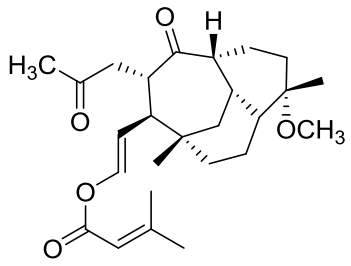	15-*O*-Methylcyclovibsanin A
46	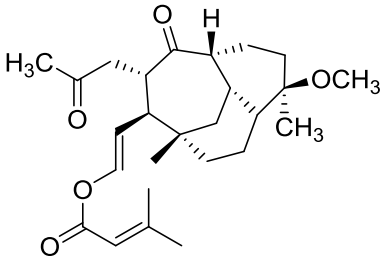	15-*O*-Methylcyclovibsanin B
47	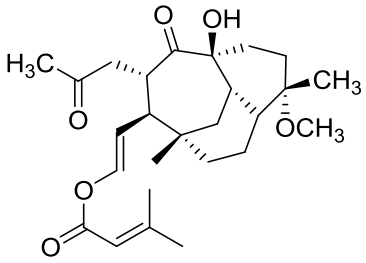	3-Hydroxy-15-*O*-methylcyclovibsanin A
48	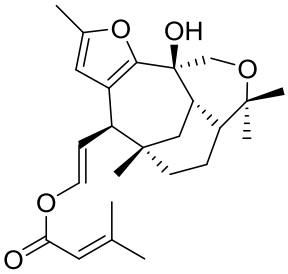	Furanovibsanin A
49	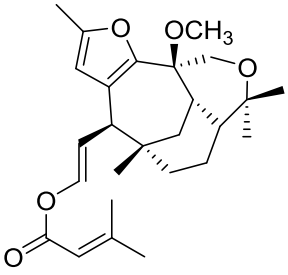	3-*O*-Methylfuranovibsanin A
50	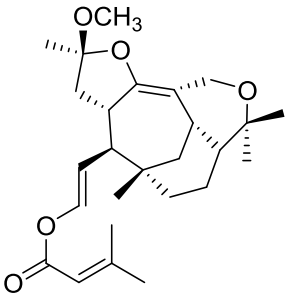	Furanovibsanin F

51	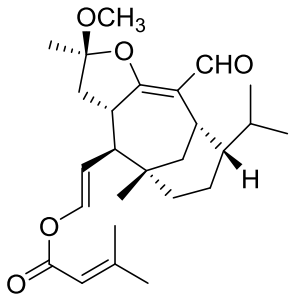	Furanovibsanin D
52	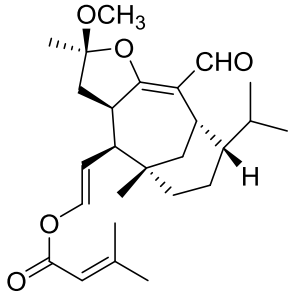	Furanovibsanin C
53	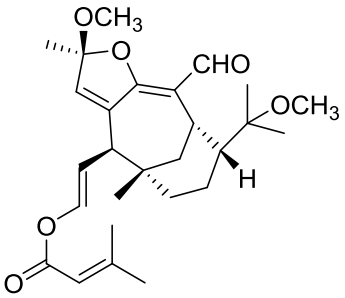	Furanovibsanin B
54	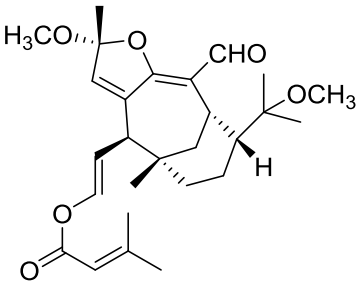	7-Epifuranovibsanin B
55	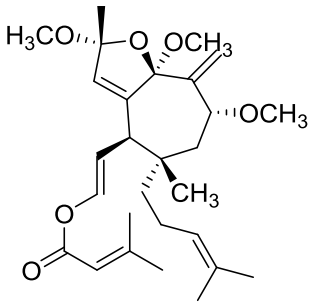	Furanovibsanin E

56	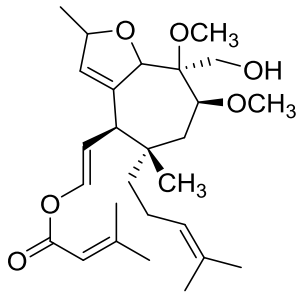	Furanovibsanin G
57	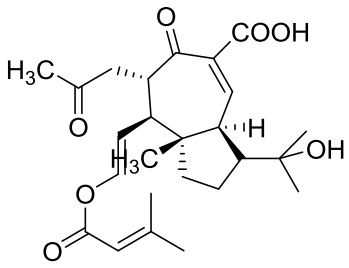	Vibsanin O
58	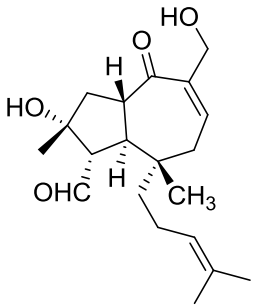	7-Epialdovibsanin A
59	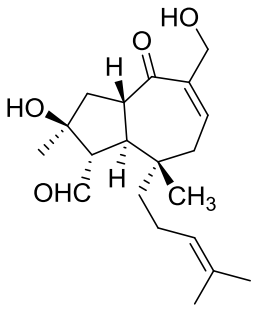	Aldovibsanin A
60	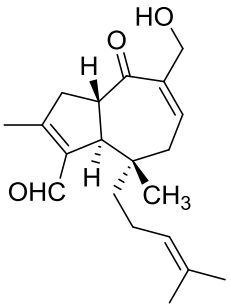	Aldovibsanin B

61	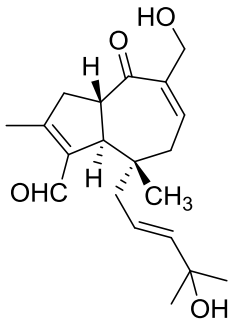	Aldovibsanin C
62	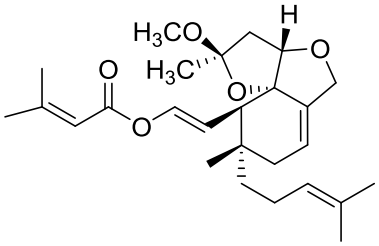	Neovibsanin A
63	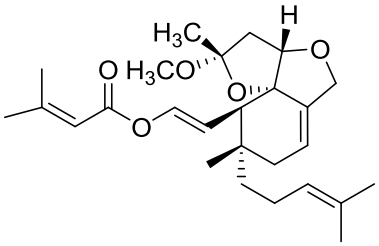	Neovibsanin B
64	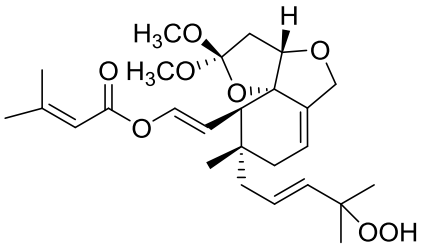	Neovibsanin D
65	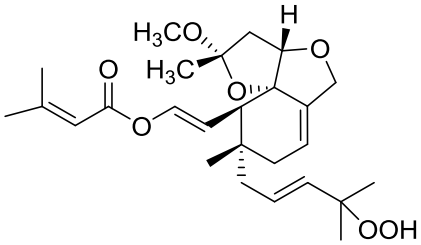	7-Epineovibsanine D
66	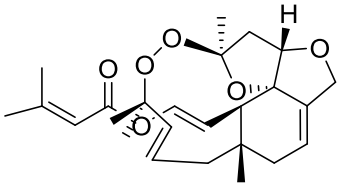	Neovibsanin C

67	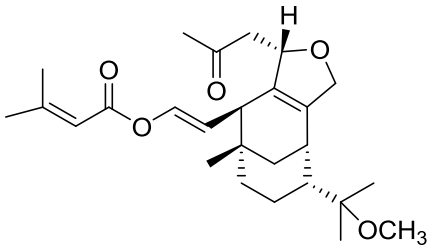	15-*O*-Methyln eovibsanin F
68	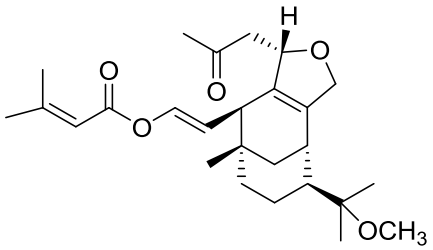	15-*O*-Methyl-14-epineovibsanin F
69	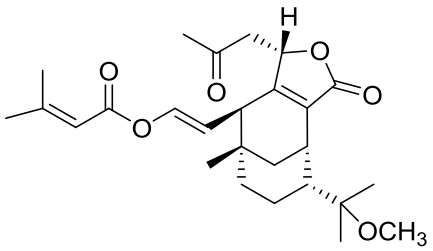	15-*O*-Methyl-18-epineovibsanin F
70	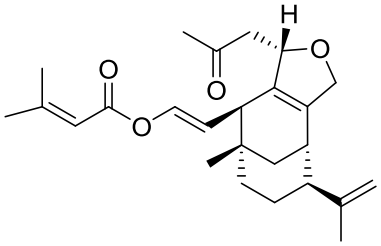	14-Epineovibsanin G
71	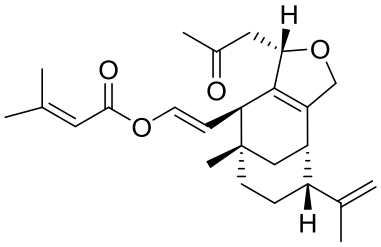	Neovibsanin G
72	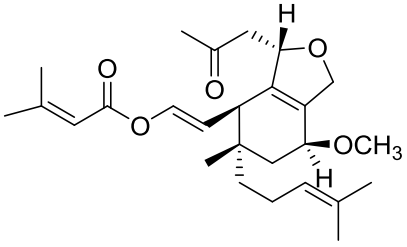	2-*O*-Methylne ovibsanin H

73	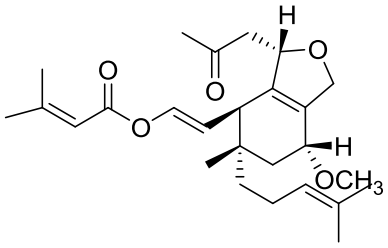	2-*O*-Methylne ovibsanin I
74	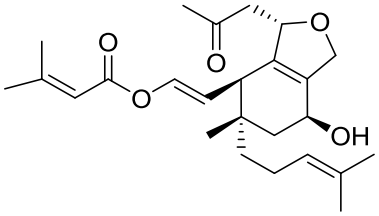	Neovibsanin H
75	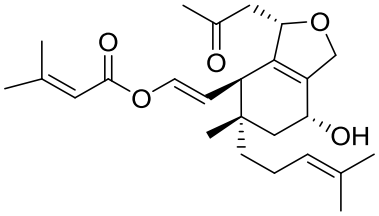	Neovibsanin I
76	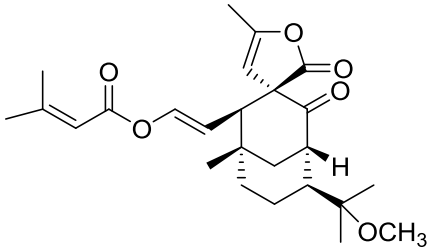	Spirovibsanin A
77	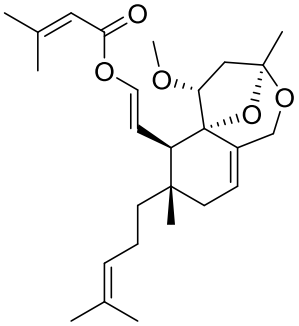	Neovibsanin J
78	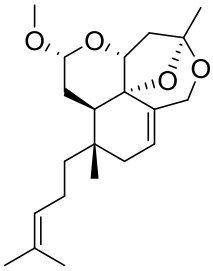	Neovibsanin K

79	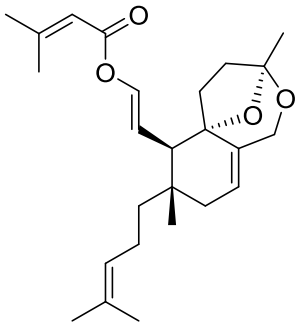	Neovibsanin P
80	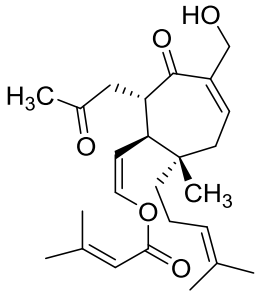	Vibsaniguration A

Table S1 Chemical ingredients database.

PDB Code	Protein name	gene name	Degree	Betweenness Centrality
5JEB	Epidermal growth factor receptor	EGFR	52	0.14144373
4OTW	Receptor tyrosine-protein kinase erbB-3	ERBB3	45	0.11649773
5OQ4	Phosphatidylinositol 4,5-bisphosphate 3-kinase catalytic subunit gamma isoform	PIK3CG	44	0.09991478
1T8I	DNA topoisomerase I	TOP1MT	40	0.09078677
5FXS	Insulin-like growth factor I receptor	IGF1R	40	0.07329712
2OWB	Serine/threonine-protein kinase PLK1	PLK1	39	0.07852847
2XVD	Ephrin type-B receptor 4	EPHB4	38	0.06066649
5E8A	Galectin-3	LGALS3	36	0.0857321
4LXD	Apoptosis regulator Bcl-2	BCL2	34	0.05499905
2Y6D	Matrilysin	MMP7	30	0.03476697
3WZD	Vascular endothelial growth factor receptor 2	KDR	26	0.02860663
1S9I	Dual specificity mitogen-activated protein kinase kinase 2	MAP2K2	22	0.02702834
2OW9	Collagenase 3	MMP13	20	0.01519915
1JK3	Macrophage metalloelastase	MMP12	16	0.01052782
4KXQ	Poly [ADP-ribose] polymerase 1	Parp1	15	0.00879503

5FTQ	ALK tyrosine kinase receptor	ALK	15	0.01335521
3ZCW	Kinesin-like protein KIF11	KIF11	10	0.0054757
4QYG	Serine/threonine-protein kinase Chk1	CHEK1	8	0.00220729
5EYD	Hepatocyte growth factor receptor	MET	6	0.00129694
5L3D	Lysine-specific histone demethylase 1A	KDM1A	6	0.00136272
4U0I	Mast/stem cell growth factor receptor	KIT	3	0.000347
1J7Y	Hemoglobin	HBA1	2	0.0000505
3HNG	Vascular endothelial growth factor receptor 1	VEGFR1	1	0

Table S2 Potential targets database.

Pathway_ID	Pathway name	Degree
hsa04151	PI3K-Akt signaling pathway	4
hsa01521	EGFR tyrosine kinase inhibitor resistance	3
hsa04068	FoxO signaling pathway	3
hsa04066	HIF-1 signaling pathway	3
hsa05200	Pathways in cancer	2
hsa05205	Proteoglycans in cancer	2
hsa04072	Phospholipase D signaling pathway	2
hsa04020	Calcium signaling pathway	2
hsa04015	Rap1 signaling pathway	2
hsa04014	Ras signaling pathway	2
hsa04012	ErbB signaling pathway	2
hsa04010	MAPK signaling pathway	2
hsa05222	Small cell lung cance	1
hsa04110	Cell cycle	1
hsa04022	cGMP-PKG signaling pathway	1
hsa04725	Cholinergic synapse	1
hsa00562	Inositol phosphate metabolism	1
hsa04722	Neurotrophin signaling pathway	1
hsa04630	Jak-STAT signaling pathway	1
hsa05206	MicroRNAs in cancer	1

hsa05225	Hepatocellular carcinoma	1
hsa04510	mTOR signaling pathway	1
hsa04217	Necroptosis	1
hsa04215	Apoptosis - multiple species	1
hsa04210	Apoptosis	1
hsa04915	Estrogen signaling pathway	1
hsa04141	Protein processing in endoplasmic reticulum	1
hsa04140	Autophagy - animal	1
hsa04064	NF-kappa B signaling pathway	1
hsa01524	Platinum drug resistance	1
hsa04310	Wnt signaling pathway	1
hsa05224	Breast cancer	1
hsa05218	Melanoma	1
hsa05215	Prostate cancer	1
hsa05214	Glioma	1
hsa05202	Transcriptional misregulation in cancer	1
hsa04152	AMPK signaling pathway	1
hsa04150	mTOR signaling pathway	1
hsa04550	Signaling pathways regulating pluripotency of stem cells	1

Table S3 The parameters of pathways.